

Electronic Supplementary Information(ESI)

for

Aminomethylpyrene-based Imino-Phenol as Primary Fluorescence Switch-on Sensors for Al³⁺ in Solution and in Vero Cells and their Complexes as Secondary Recognition Ensemble toward Pyrophosphate

Ajit Kumar Mahapatra^{*,a}, Syed Samim Ali,^a Kalipada Maiti,^a Saikat Kumar Manna,^a Rajkishor Maji,^a Sanchita Mondal,^a Md. Raihan Uddin,^b Sukhendu Mandal^b and Prithidipa Sahoo^c

^aDepartment of Chemistry, Indian Institute of Engineering Science and Technology, Shibpur, Howrah-711103, West Bengal, India.

^bDepartment of Microbiology, University of Calcutta, Kolkata- 700019.

^cDepartment of Chemistry, Visva-Bharati (A Central University), Santiniketan 731235, India.

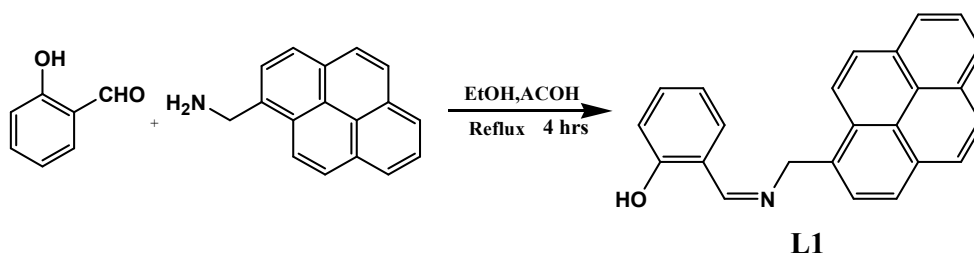
*Corresponding author: Tel.: +91 33 2668 4561; fax: +91 33 26684564;

E-mail: mahapatra574@gmail.com

General procedure for drawing Job plot by Fluorescence method:

Stock solution of similar concentration of the receptors and the guest were prepared in the order of ca. $1.0 \times 10^{-4} \text{ mL}^{-1}$ DMSO-H₂O (2:1 v/v). The fluorescence intensity in each case with different host-guest ratio but the sum of the volume of the host and guest solutions maintained constant. Job plots were drawn by plotting the spectral changes of **L1**, **L2** and **L3** at 377 nm, 416 nm and 377 nm vs volume ratio of host and guest. The total $[\text{Al}^{3+}] + [\text{L}] = 1.0 \times 10^{-4} \text{ M}$.

Synthetic Procedure:



Scheme 1: Synthesis of **L1**.

Preparation of L1:

An ethanolic solution (3 mL) of pyrenemethylamine (250 mg, 1.0 mmol) was added to another ethanolic solution (3 mL) of salicylaldehyde (122.0 mg, 1.0 mmol). The mixed solution was refluxed for 4 hrs and then cooled to room temperature. A yellow precipitate was appeared, filtered, washed with EtOH for several times and then dried under vacuum. Yellow solid. 86%. m.p: 176–180°C. **¹H-NMR** (DMSO-d₆, 400 MHz): δ (ppm) 13.47 (s, 1H), 8.88 (s, 1H), 8.50 (d, 1H, $J = 9.28 \text{ Hz}$), 8.30-8.35 (m, 4H), 8.20 (d, 2H, $J = 8.48 \text{ Hz}$), 8.08-8.12 (m, 2H), 7.49 (d, 1H, $J = 6.48 \text{ Hz}$), 7.33 (t, 1H, $J = 8.16 \text{ Hz}$), 6.91 (t, 1H, $J = 7.20 \text{ Hz}$), 6.83 (d, 1H, $J = 8.16 \text{ Hz}$), 5.57 (s, 2H). **¹³C NMR** (d₆-DMSO, 100 MHz) δ (ppm): 60.78, 117.34, 119.59, 119.70, 124.11, 124.83, 125.07, 125.97, 126.19, 126.29, 127.24, 127.86, 128.13, 128.27, 128.75, 129.22, 131.21, 131.30, 131.70, 132.65, 133.22, 133.35, 161.31, 167.34. **MS (LCMS)**: (m/z, %): **336.4144** [(L1+H⁺), 100 %]; Calculated for C₂₄H₁₇NO: **335.4012**.



Figure S1. ESI-MS of L1.

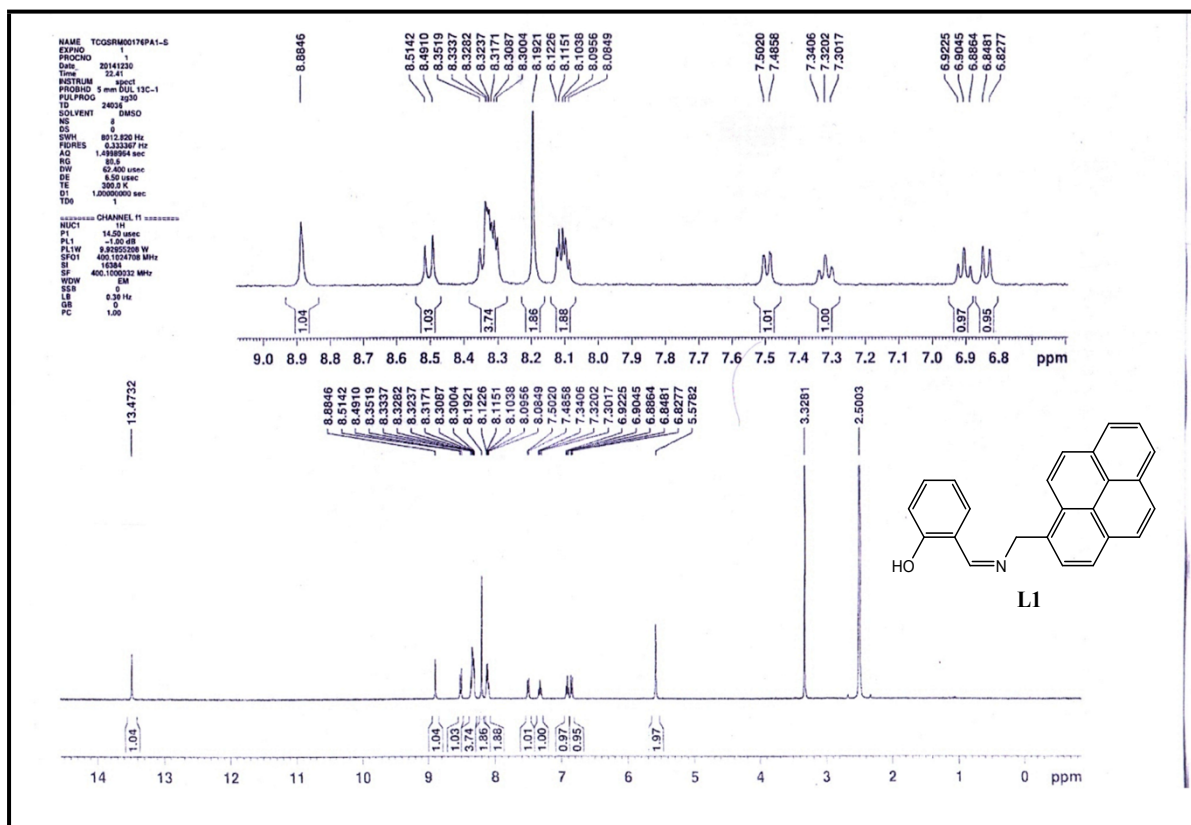


Figure S2. ^1H NMR spectra of L1.

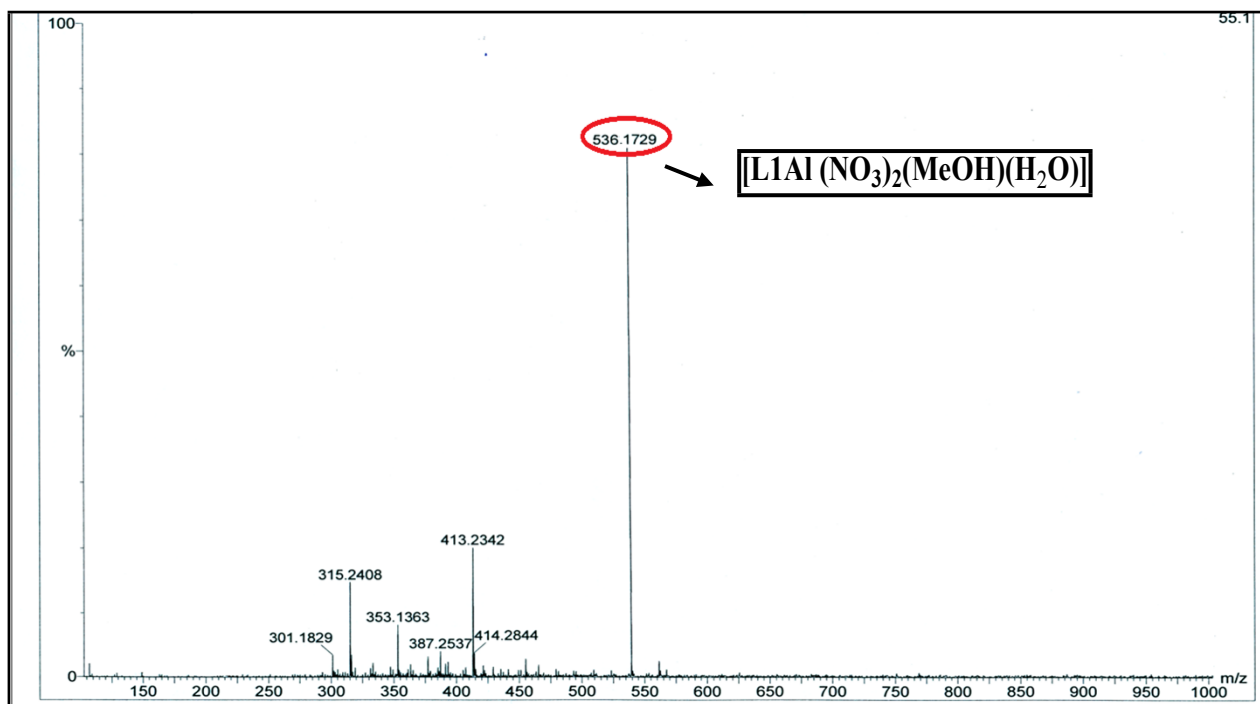
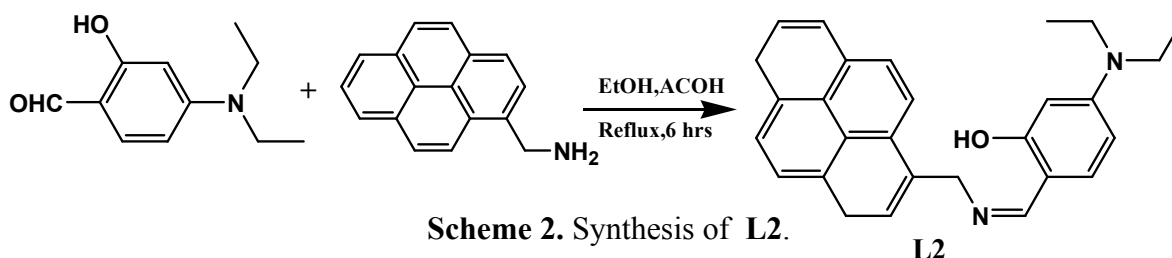


Figure S3. ESI-MS of L1- Al³⁺ complex.

Synthetic Procedure:



Preparation of L2:

An ethanolic solution (3 mL) of pyrenemethylamine (250 mg, 1.0 mmol) was added to another ethanolic solution (3 mL) of 4-N,N-diethyl amino salicylaldehyde (193.0 mg, 1.0 mmol). The mixed solution was refluxed for 6 hrs and then cooled to room temperature. A yellow precipitate was appeared, filtered, washed with EtOH for several times and then dried under vacuum. Yellow solid. 78%. m.p: 176–180°C. ¹H-NMR (DMSO-d₆, 400 MHz): δ (ppm) 13.76 (s, 1H), 8.56 (s, 1H), 8.47 (d, 1H, *J* = 9.2 Hz), 8.28-8.33 (m, 4H), 8.19 (s, 2H), 8.07-8.12 (m, 2H), 7.16 (d, 1H, *J* = 8.8 Hz), 6.20 (d, 1H, *J* = 8.8 Hz), 5.96 (d, 1H, *J* = 8.0 Hz), 5.44 (s, 2H), 3.29-3.38 (m, 4H), 1.05-1.09 (t, 6H, *J* = 13.6 Hz). ¹³C NMR (d₆-DMSO, 100 MHz) δ (ppm): 13.09, 25.74, 59.21, 97.78, 103.60, 108.60, 123.87, 124.54, 124.74, 125.63, 125.84, 125.94, 126.92, 127.32,

127.73, 127.99, 128.32, 128.79, 130.85, 130.92, 131.41, 133.69, 151.53, 164.74, 165.35.
MS (LCMS): (m/z, %): 408.5 [(L2+H⁺), 100 %]; Calculated for C₂₈H₂₈N₂O: 408.22.

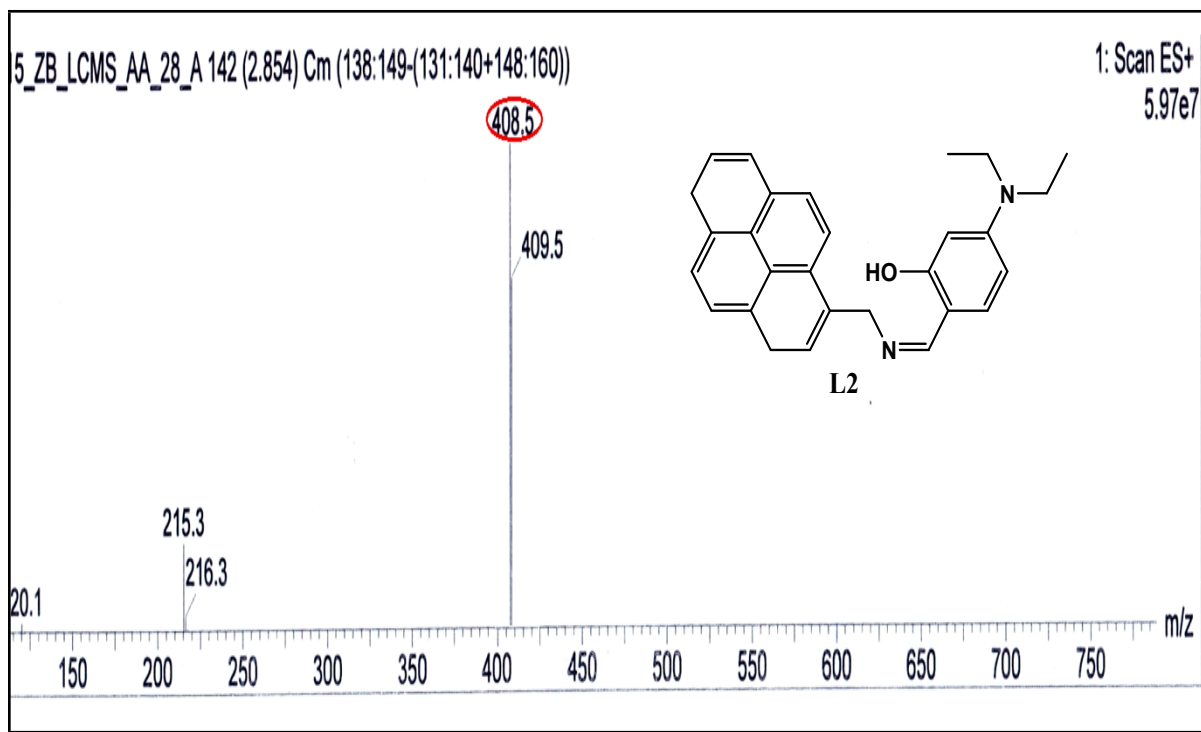


Figure S4. LC-MS of L2.

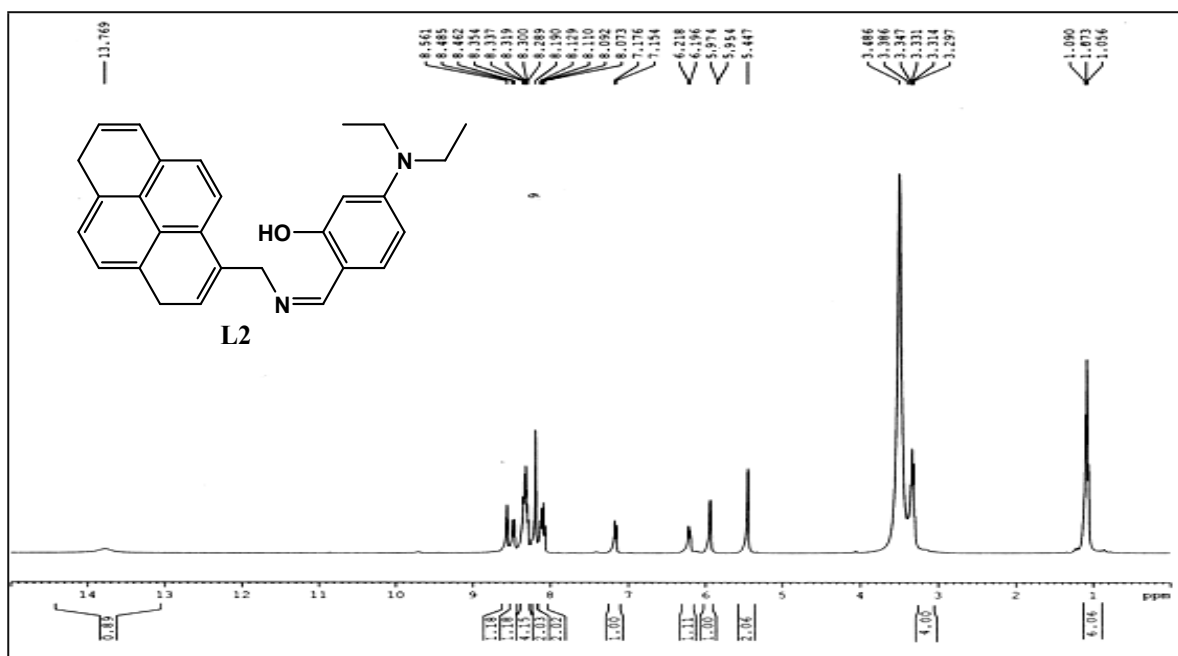


Figure S5. ¹H NMR spectra of L2.

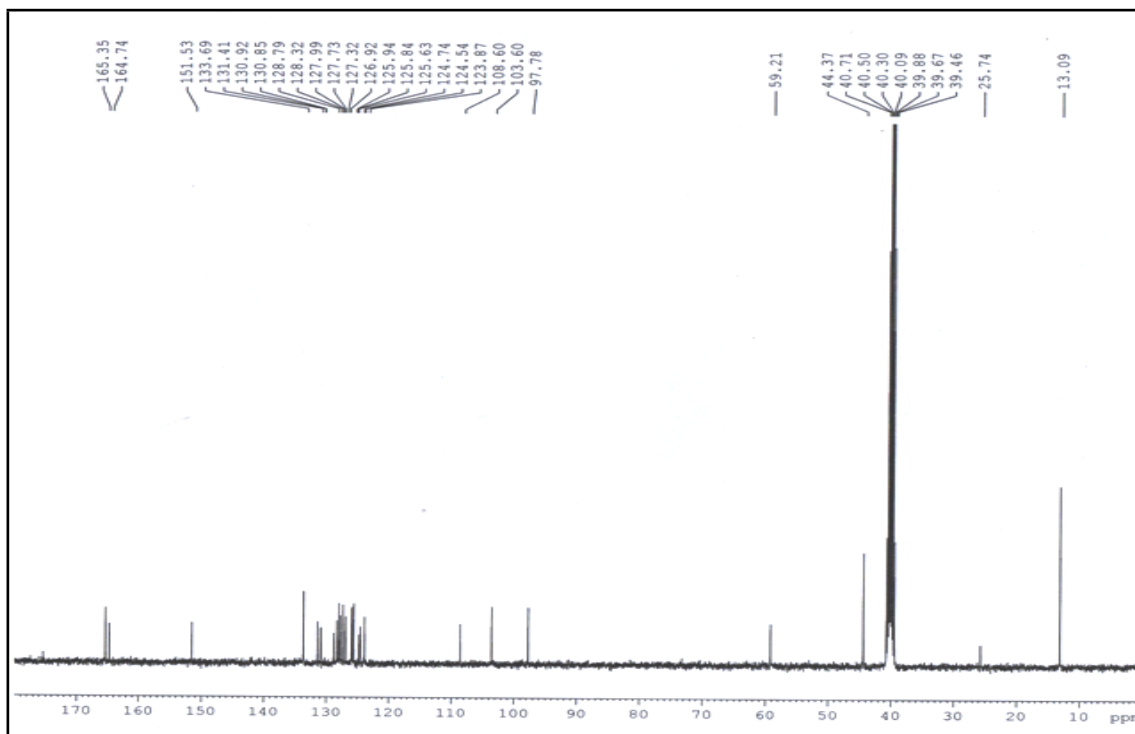


Figure S6. ^{13}C NMR spectra of L2.

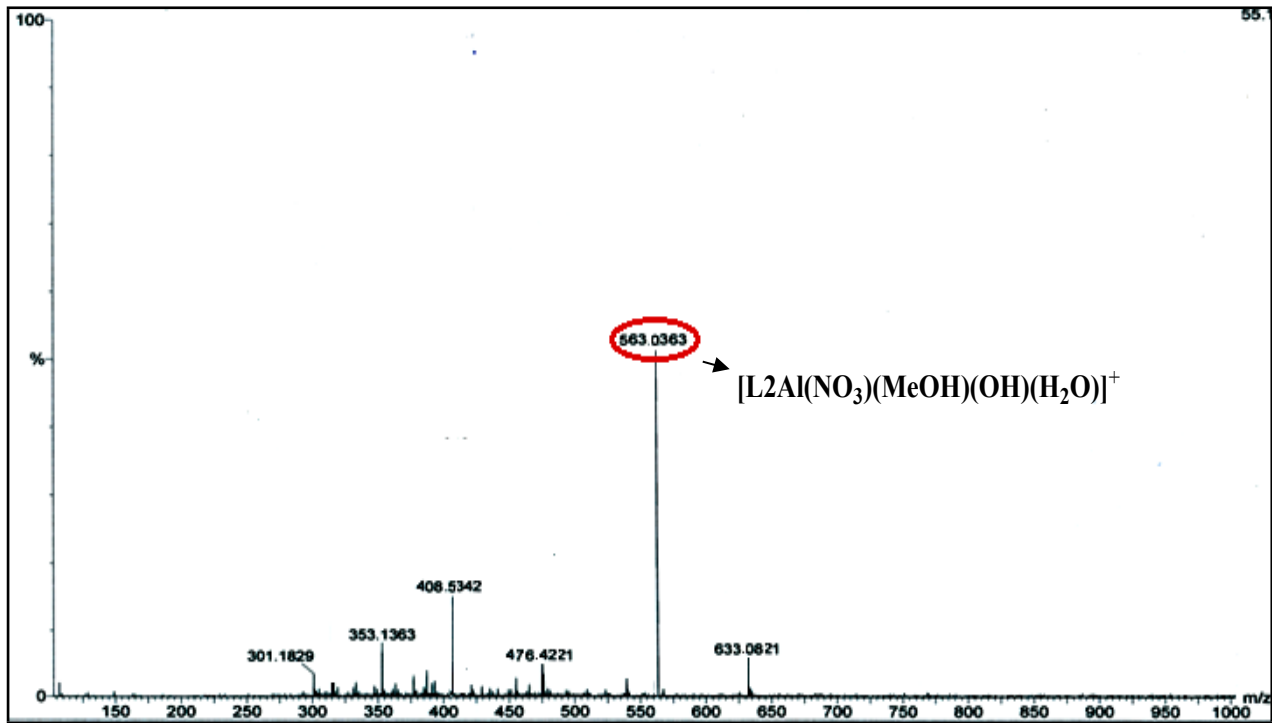
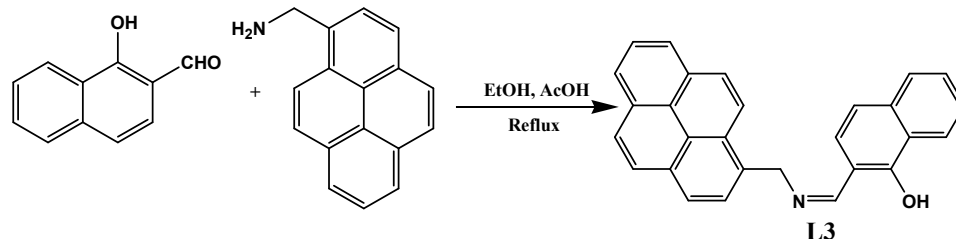


Figure S7. HRMS spectra of L2- Al^{3+} complex.

Synthetic Procedure:



Scheme 3. Synthesis of L3.

Preparation of L3:

An ethanolic solution (3 mL) of pyrenemethylamine (250 mg, 1.0 mmol) was added to another ethanolic solution (3 mL) of 1-hydroxy-2-naphthaldehyde (172.8 mg, 1.0 mmol). The mixed solution was refluxed for 6 hrs and then cooled to room temperature. A yellow precipitate was appeared, filtered, washed with EtOH for several times and then dried under vacuum. Yellow solid. 82%. m.p: 176–180°C. ¹H-NMR (DMSO-d₆, 400 MHz): δ (ppm) 13.53 (s, 1H), 8.68 (s, 1H), 8.54 (d, 1H, *J* = 9.24 Hz), 8.33-8.37 (m, 4H), 8.18-8.21 (m, 4H), 8.10-8.14 (m, 1H), 7.59 (d, 1H, *J* = 7.92 Hz), 7.52 (t, 1H, *J* = 14.4 Hz), 7.33 (t, 1H, *J* = 14.8 Hz), 7.10 (d, 1H, *J* = 8.84 Hz), 6.73 (d, 1H, *J* = 8.84 Hz), 5.58 (d, 2H). ¹³C NMR (d₆-DMSO, 100 MHz) δ (ppm): 52.47, 109.42, 113.96, 123.74, 124.77, 125.50, 125.78, 126.10, 126.43, 126.55, 127.41, 127.96, 128.05, 128.28, 128.51, 129.16, 129.24, 129.92, 130.68, 131.04, 131.19, 131.71, 138.23, 163.23. MS (LCMS): (m/z, %): 386.0 [(L3+H⁺), 100 %]; Calculated for C₂₈H₁₉NO: 385.15

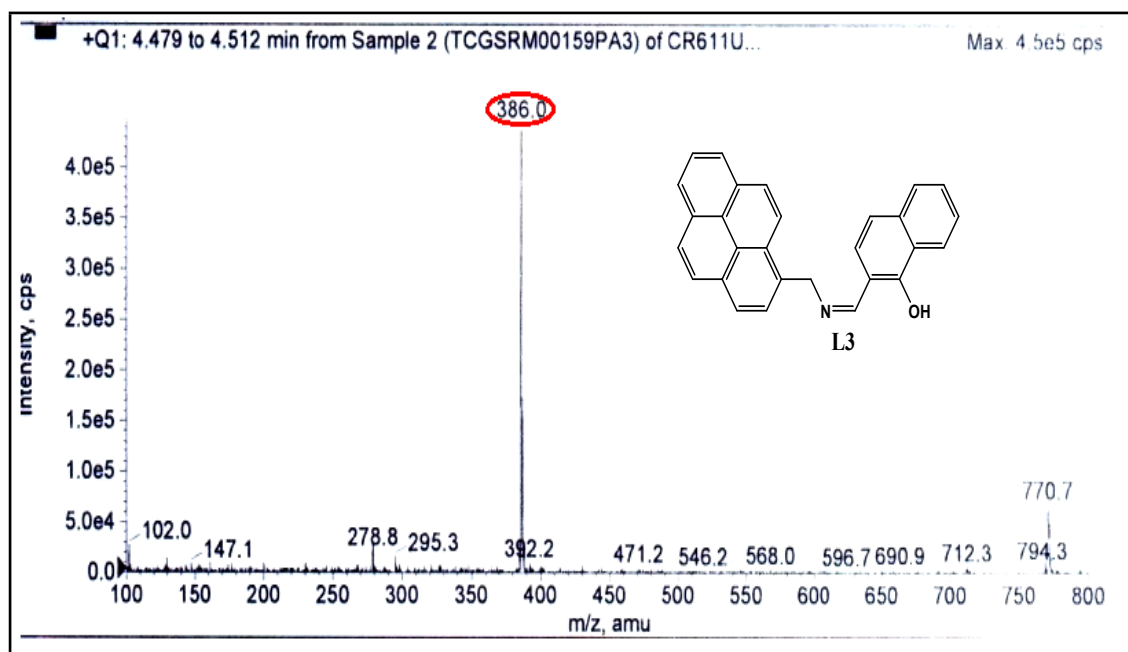


Figure S8. LC-MS of L3.

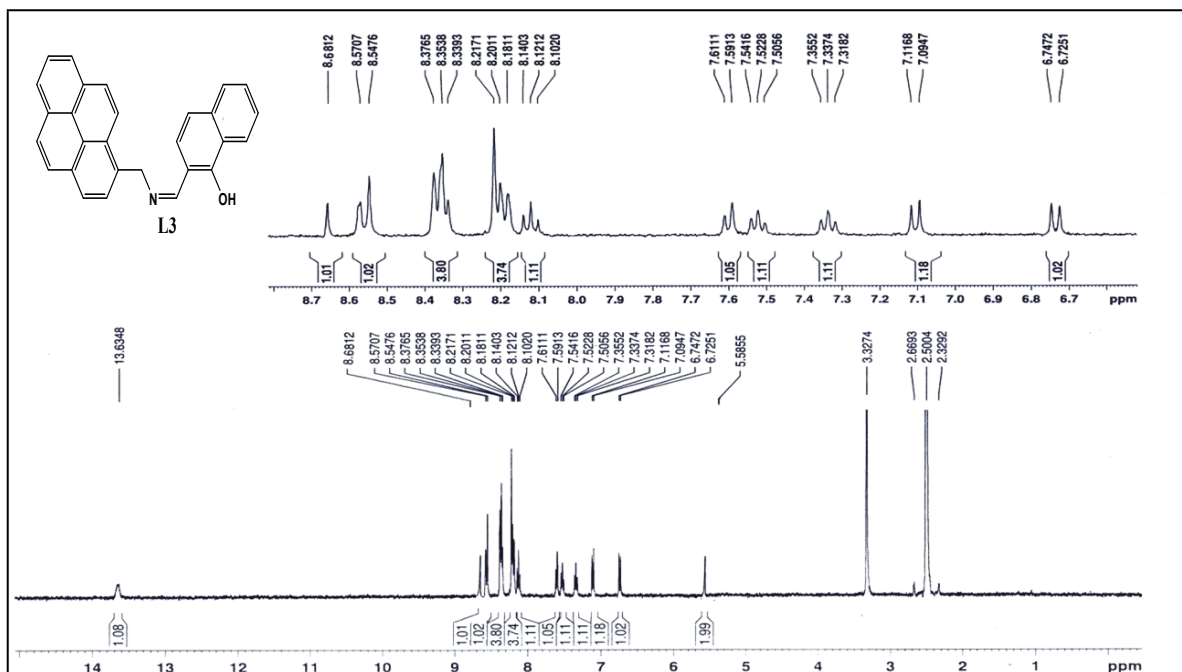


Figure S9. ^1H NMR spectra of L3.

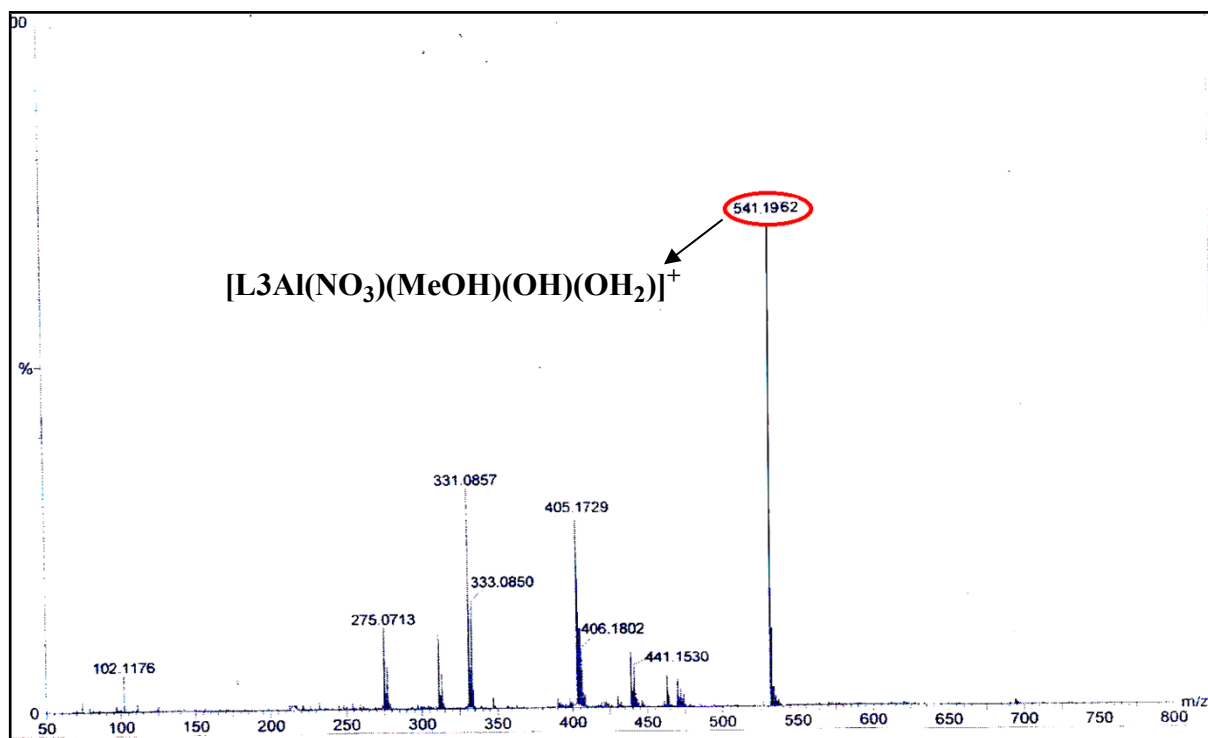


Figure S10. ESI-MS of L3- Al^{3+} complex.

Table S1. Binding constant and detection limit of **L1**, **L2**, **L3**.

Compound	Binding constant	Std. deviation	Detection limit
L1	2×10^4 (M)	24.35586	3.6 μ M
L2	4.1×10^4 (M)	28.88453	2.13 μ M
L3	1.9×10^4 (M)	14.22561	2.16 μ M

Calculations for detection limit:

The detection limit (DL) of **L1**, **L2** and **L3** for Al^{3+} .were determined from the following equation:

$$DL = K * Sb1/S$$

Where $K = 2$ or 3 (we take 3 in this case); $Sb1$ is the standard deviation of the blank solution; S is the slope of the calibration curve.

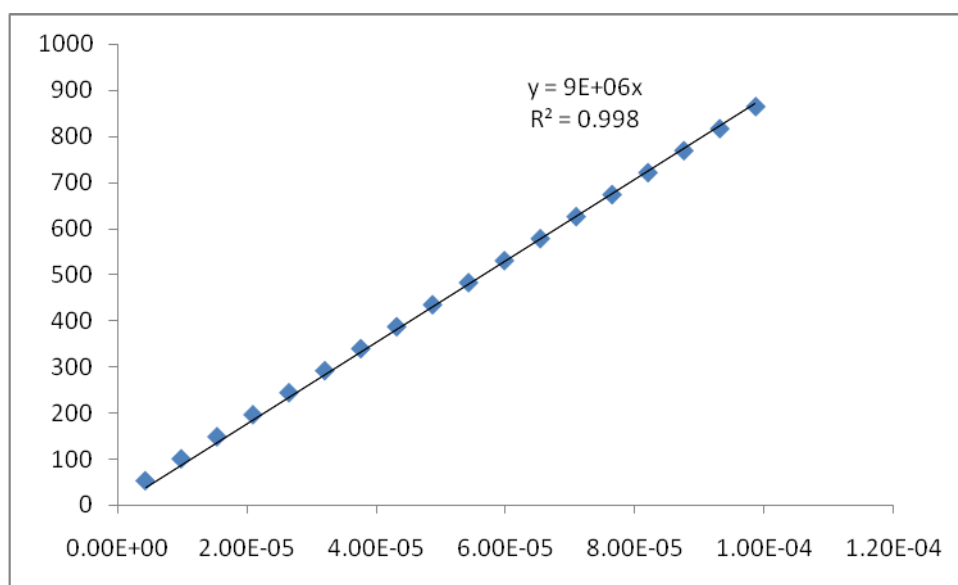


Figure S11. Graph for the calculation of detection limit of Al^{3+} towards **L1**.

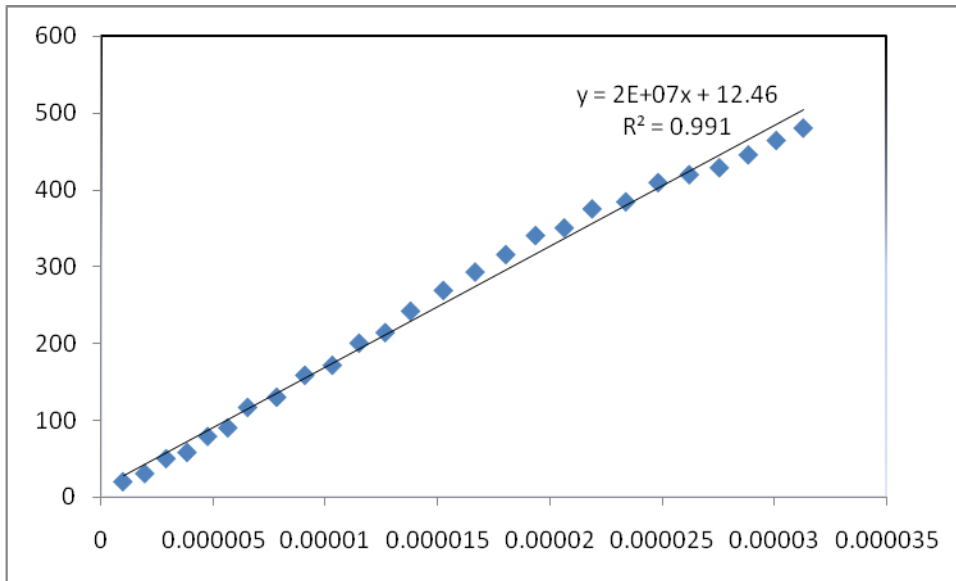


Figure S12. Graph for the calculation of detection limit of Al^{3+} towards **L2**.

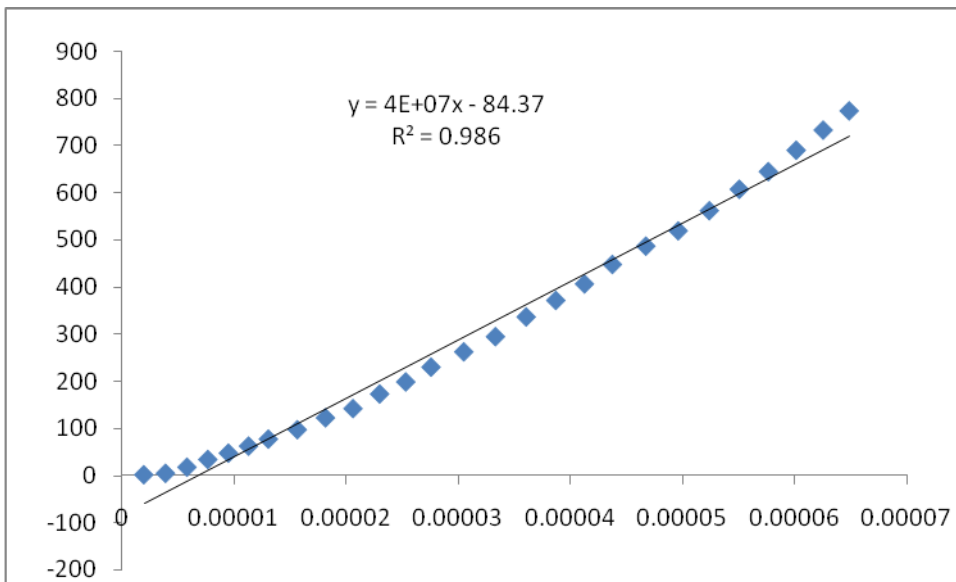


Figure S13. Graph for the calculation of detection limit of Al^{3+} towards **L3**.

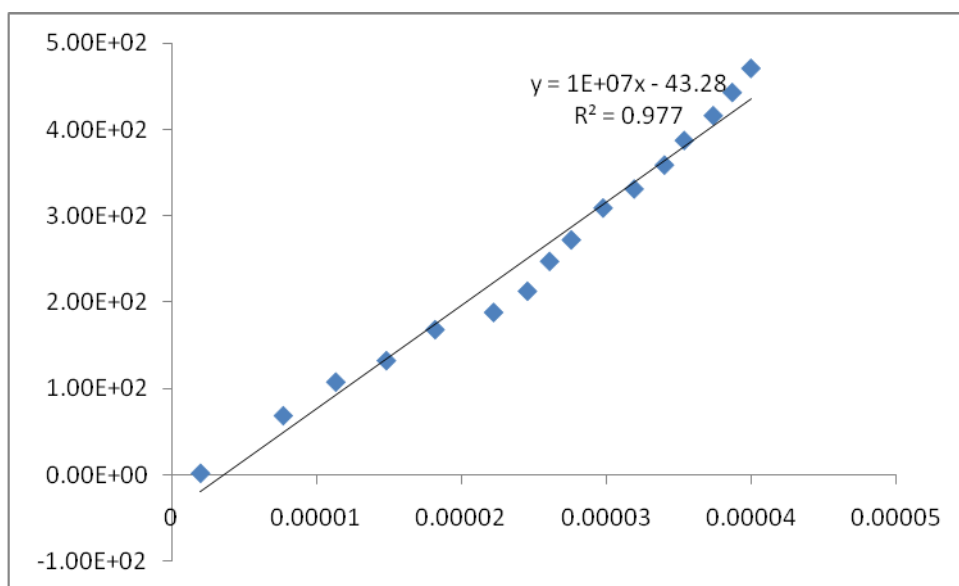


Figure S14. Graph for the calculation of detection limit of **PPI** towards[**Al-L3**].

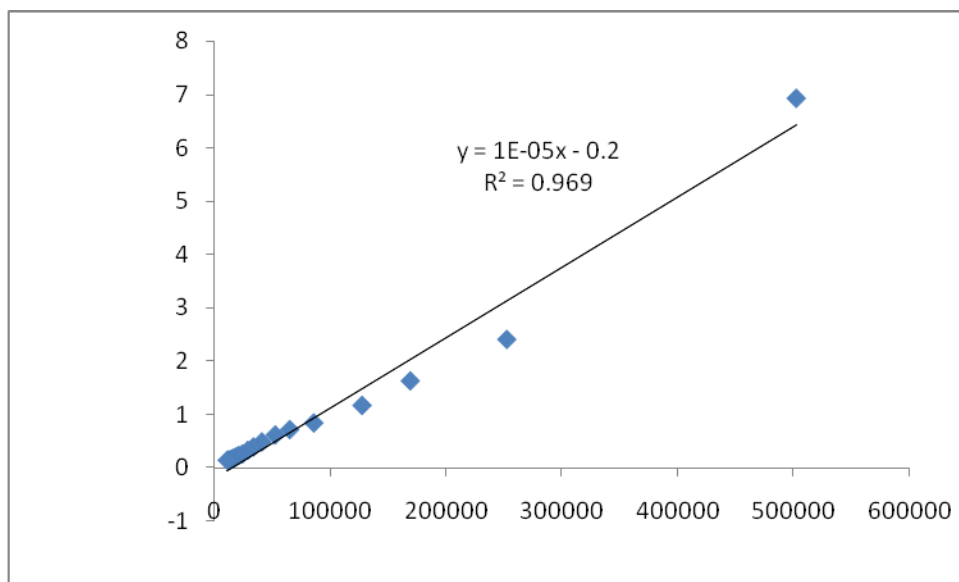


Figure S15. Graph for the calculation of binding constant of **L1**.

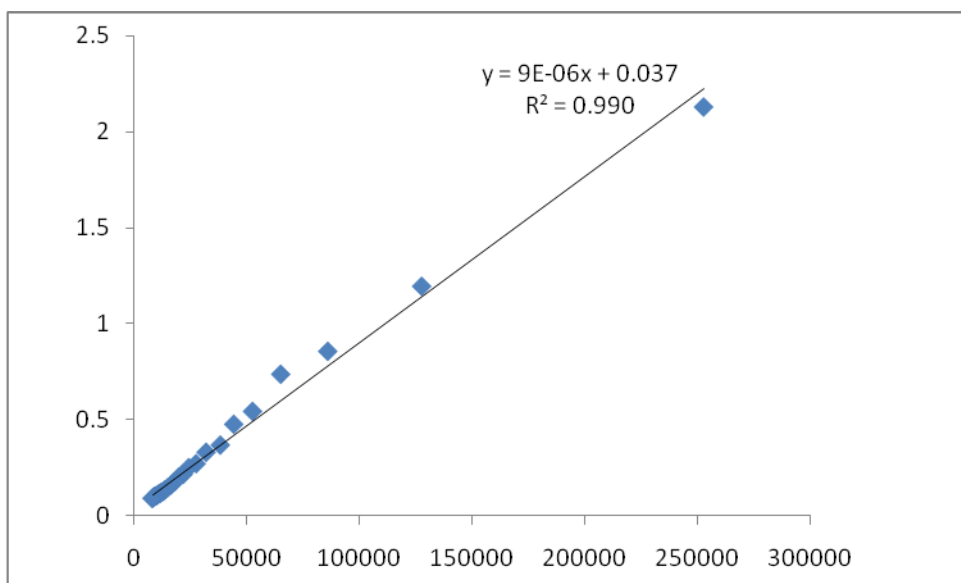


Figure S16. Graph for the calculation of binding constant of **L2**.

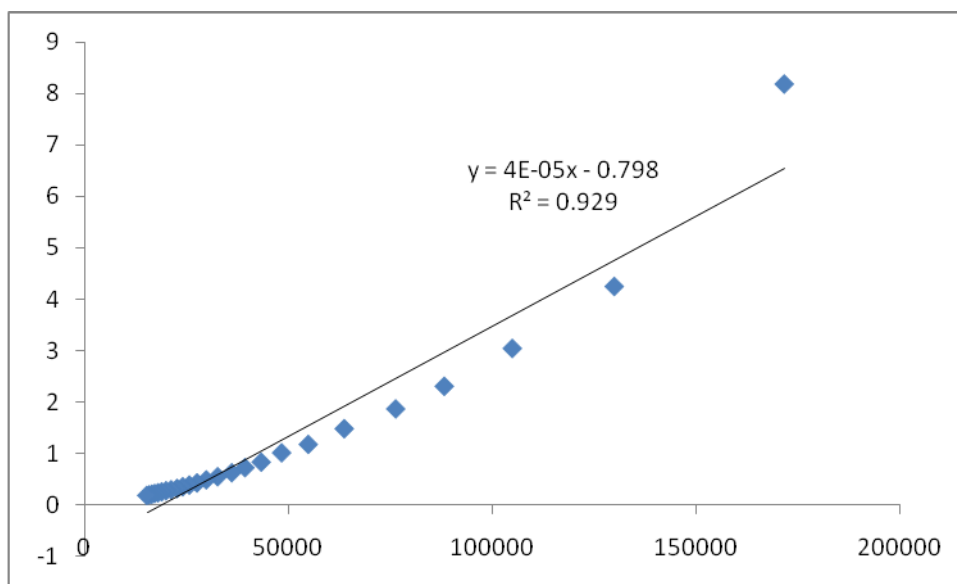


Figure S17. Graph for the calculation of binding constant of **L3**.

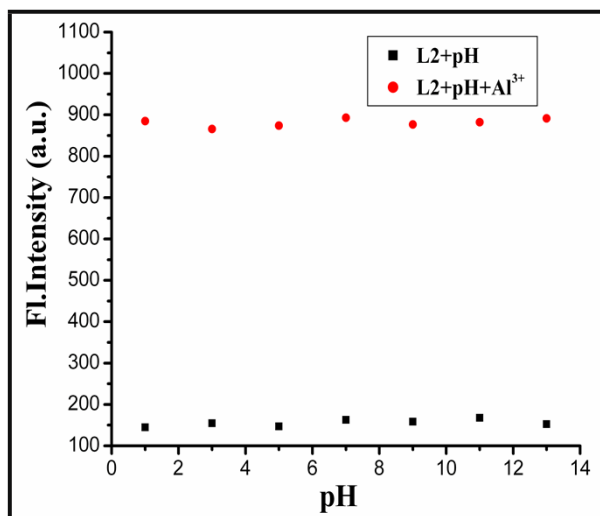


Figure S18. Change in fluorescence intensity ($\lambda_{\text{ex}}=351\text{ nm}$) of **L2** (at 416 nm) with different pH (black dots) and with the addition of Al^{3+} in to it (red dots).

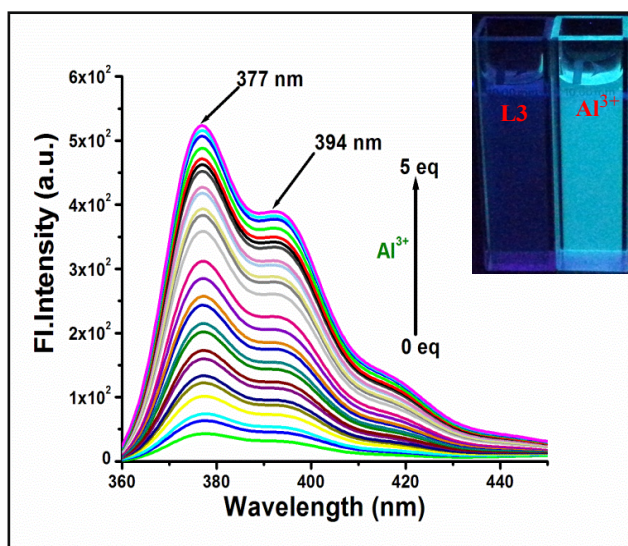


Figure S19. Fluorescence changes of **L3** ($2.0 \times 10^{-5}\text{ M}$) in $\text{DMSO-H}_2\text{O}$ (2:1, v/v; pH 7.4) upon addition of Al^{3+} ($4.0 \times 10^{-4}\text{ M}$). The inset shows naked eye color change of **L3** and addition of Al^{3+} in $\text{DMSO-H}_2\text{O}$ (2:1, v/v; pH 7.4).

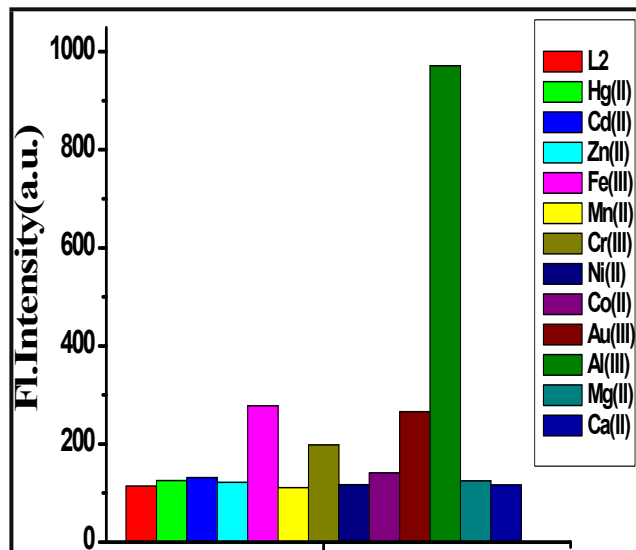


Figure S20. Change in fluorescence intensity of **L2** (2.0×10^{-5} M) in DMSO-H₂O (2:1, v/v; pH 7.4) at 416 nm ($\lambda_{\text{ex}} = 351$ nm) in presence of different metal ions (4.0×10^{-4} M).

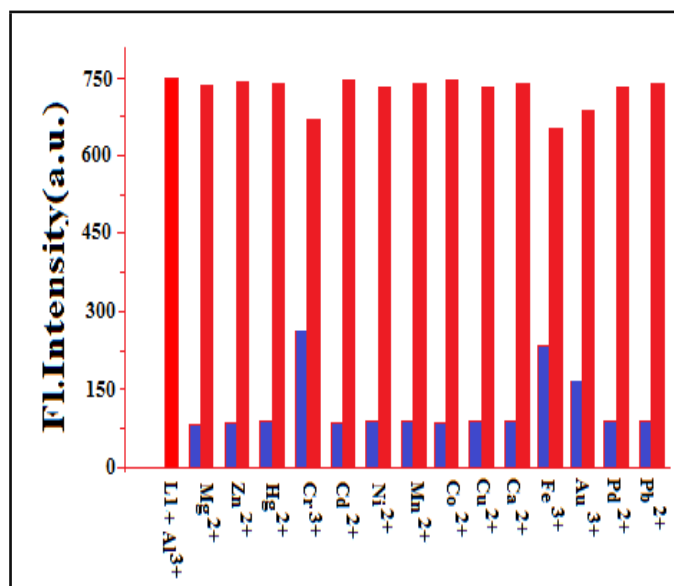


Figure S21. Competitive graph; blue bar: **L1** + cations (5 equiv.), red bar: **L1** + cations (5 equiv.) + Al³⁺ (3 equiv.).

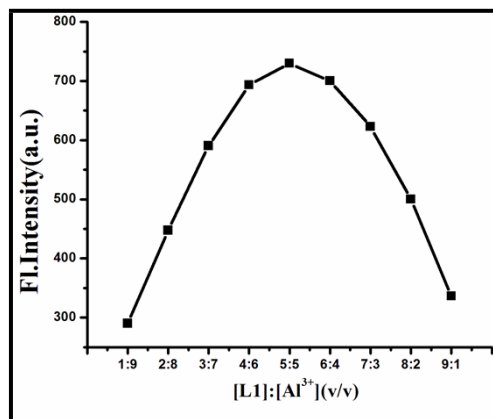


Figure S22. Fluorescence Job's plot of L1 with Al³⁺.

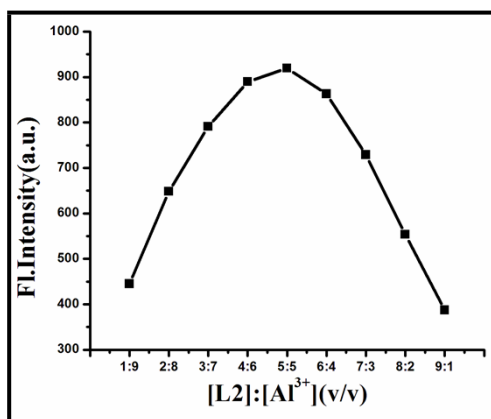


Figure S23. Fluorescence Job's plot of L2 with Al³⁺.

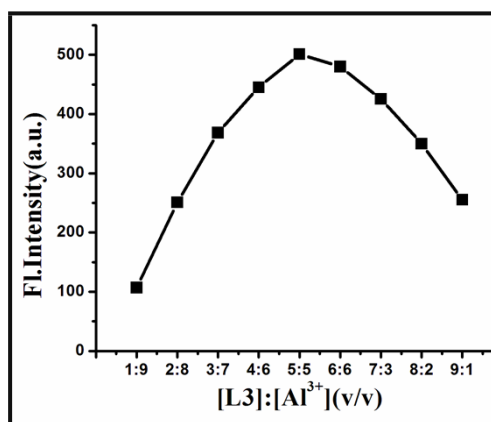


Figure S24. Fluorescence Job's plot of L3 with Al³⁺.

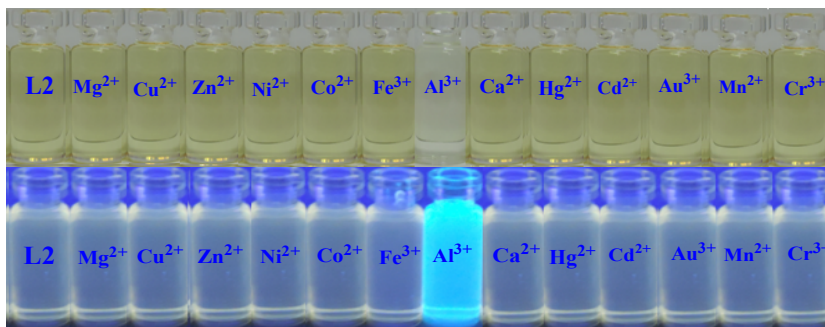


Figure S25. The visible color (top) and fluorescence changes (bottom) of receptor **L2** in aq. DMSO (DMSO: H₂O = 7:3 v/v, 20 mM HEPES buffer, pH = 7.4) upon addition of various cations.

16. Computational Method:

Geometries have been optimized in B3LYP density functional method with 6-31+G (d) basis set for all atom. The geometries are verified as proper minima or not by frequency calculations. Time-dependent density functional theory calculation has also been performed at the same level of theory.

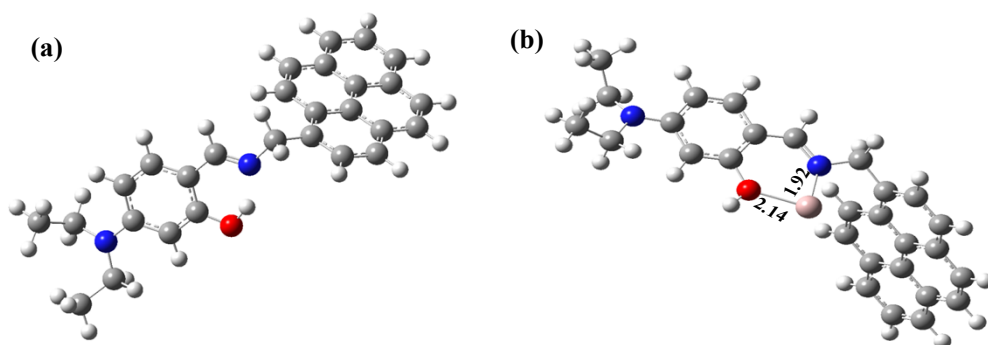


Figure S26. Energy minimization structure of (a) **L2** and (b) **[AIL2]**.

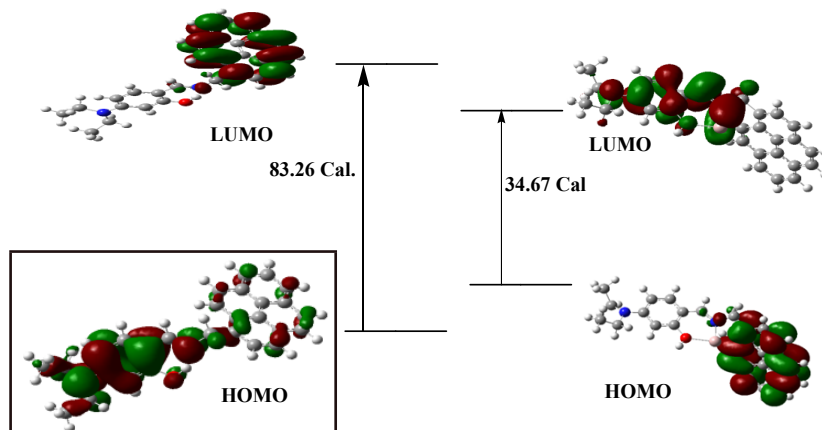


Figure S27. HOMO and LUMO orbitals energy diagram of **L2** and **[AIL2]** complex.

Table S2. HOMO-LUMO energy calculated data of **L2** and **L2•Al** complex

Species	E(HOMO)	E(LUMO)	ΔE (Hartree)	ΔE (eV)	ΔE (kcal/mol)
L2	-0.18729	-0.05460	0.13269	3.6107602	83.2643090
L2•Al complex	-0.11050	-0.05525	0.055250	1.5034630	34.66992750
	E(HOMO-1)	E(LUMO+1)	ΔE (Hartree)	ΔE (eV)	ΔE (kcal/mol)
L2	-0.19385	-0.03095	0.16290	4.4328348	102.2213790
L2•Al complex	-0.17551	-0.02191	0.153600	4.1797632	96.3855360
	E(HOMO-2)	E(LUMO+2)	ΔE (Hartree)	ΔE (eV)	ΔE (kcal/mol)
L2	-0.21158	-0.01900	0.192580	5.24048696	120.8458758
L2•Al complex	-0.19570	-0.01197	0.183730	4.9996607	115.2924123

Table S3. Selected electronic excitation energies (eV), oscillator strengths (f), main configurations, and CI Coefficients of the low-lying excited states of **L2**. The data were calculated by TDDFT//B3LYP/6-31+G(d) based on the optimized ground state geometries.

λ (nm)	E (eV)	Osc. Strength (f)	Key Excitations
392.22	3.16	0.0431	(99.17%)HOMO→LUMO
349.78	3.54	0.5411	(88.5%)HOMO-1 → LUMO
331.55	3.74	0.0275	(26.23%) HOMO-1 → LUMO+1 (24.08%) HOMO-1 → LUMO+2 (7.24%) HOMO → LUMO+1 (3.32%) HOMO → LUMO+2

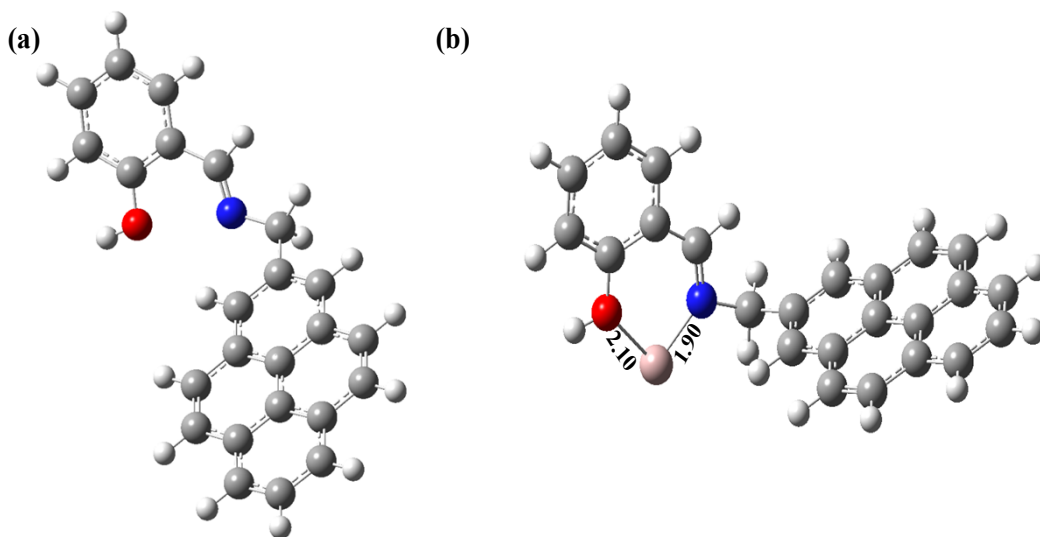


Figure S28. Energy minimization structure of (a) L1 and (b) [AIL1].

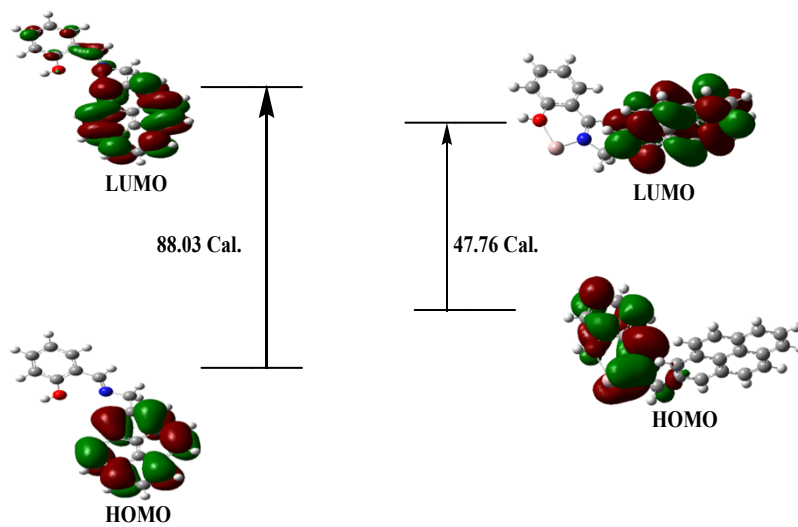


Figure S29. HOMO and LUMO orbitals energy diagram of L1 and [AIL1] complex.

Table S4. HOMO-LUMO energy calculated data of **L1** and **L1•Al** complex

Species	E(HOMO)	E(LUMO)	ΔE (Hartree)	ΔE (eV)	ΔE (kcal/mol)
L1	-0.18904	-0.04875	0.14029	3.817571	88.03337
L1•Al complex	-0.13083	-0.05472	0.07611	2.071105	47.7597
	E(HOMO-1)	E(LUMO+1)	ΔE (Hartree)	ΔE (eV)	ΔE (kcal/mol)
L1	-0.21717	-0.03957	0.17760	4.8328512	111.4457760
L1•Al complex	-0.19552	-0.03020	0.16532	4.4986878	103.7399532
	E(HOMO-2)	E(LUMO+2)	ΔE (Hartree)	ΔE (eV)	ΔE (kcal/mol)
L1	-0.22457	-0.01553	0.20904	5.688396480	131.1746904
L1•Al complex	-0.19686	-0.02323	0.17362	4.72454744	108.948286

Table S5. Selected electronic excitation energies (eV), oscillator strengths (f), main configurations, and CI Coefficients of the low-lying excited states of **L1**. The data were calculated by TDDFT//B3LYP/6-31+G(d) based on the optimized ground state geometries

λ (nm)	E (eV)	Osc. Strength (f)	Key Excitations
343.91	3.61	0.4885	(92.74%)HOMO→LUMO
331.00	3.75	0.0006	(48.34%)HOMO-2 → LUMO (5.00%) HOMO-1 → LUMO (45.77%) HOMO → LUMO+2
317.41	3.91	0.0087	(98.09%) HOMO→ LUMO+1

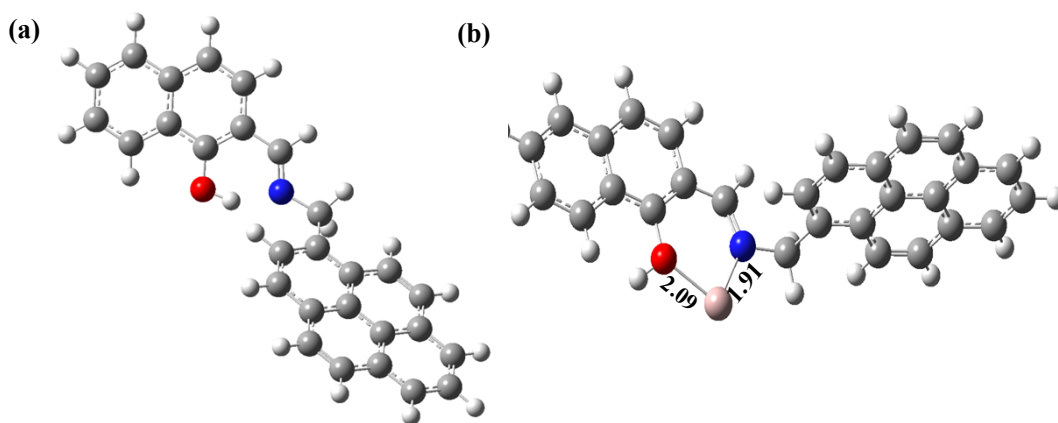


Figure S30. Energy minimization structure of (a) L3 and (b) [AIL3].

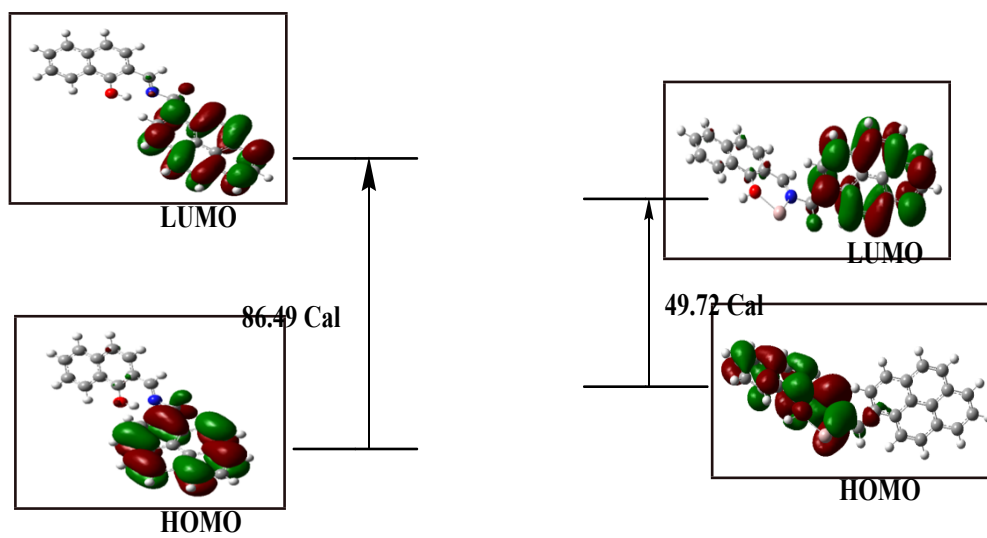


Figure S31. HOMO and LUMO orbitals energy diagram of L3 and [AIL3] complex .

Table S6. HOMO-LUMO energy calculated data of **L3** and **L3•Al** complex.

Species	E(HOMO)	E(LUMO)	ΔE (Hartree)	ΔE (eV)	ΔE (kcal/mol)
L3	-0.19497	-0.05713	0.137348	3.75090	86.495978
L3•Al complex	-0.13592	-0.05668	0.07924	2.1562788	49.7238924
	E(HOMO-1)	E(LUMO+1)	ΔE (Hartree)	ΔE (eV)	ΔE (kcal/mol)
L3	-0.20141	-0.05450	0.14691	3.9977	92.18749
L3•Al complex	-0.19402	-0.04140	0.15262	4.15309544	95.77057620
	E(HOMO-2)	E(LUMO+2)	ΔE (Hartree)	ΔE (eV)	ΔE (kcal/mol)
L3	-0.22879	-0.02406	0.20473	5.5711	128.4701223
L3•Al complex	-0.19947	-0.02510	0.174370	4.74495644	109.4189197

Table S7. Selected electronic excitation energies (eV), oscillator strengths (*f*), main configurations, and CI Coefficients of the low-lying excited states of **L1**. The data were calculated by TDDFT//B3LYP/6-31+G(*d*) based on the optimized ground state geometries.

λ (nm)	E (eV)	Osc. Strength <i>f</i>	Key Excitations
362.9	3.42	0.1630	(18.73%)HOMO→LUMO (78.42%) HOMO → LUMO+1
355.72	3.49	0.4954	(61.62%)HOMO → LUMO
346.79	3.58	0.0506	(76.39%) HOMO-1 → LUMO+1

Cytotoxic effect on Cells:

The cytotoxic effects of **L2**, **Al** and [**AIL2**] complex were determined by MTT assay following the manufacturer's instruction (MTT 2003, Sigma-Aldrich, MO). Vero cells were seeded onto 96-well plates (approximately 104 cells per well) for 24 h. Next day media was removed and various concentrations of probe **L2**, **Al** (0, 0.625, 1.25, 2.50 and 5.0 μ M) made in DMEM were

added to the cells and incubated for 24 h. Solvent control samples (cells treated with DMSO in DMEM), no cells and cells in DMEM without any treatment were also included in the study. Following incubation, the growth media was removed, and fresh DMEM containing MTT solution was added. The plate was incubated for 3–4 h at 37°C. Subsequently, the supernatant was removed, the insoluble colored formazan product was solubilized in DMSO, and its absorbance was measured in a microtiter plate reader (Perkin-Elmer) at 570.

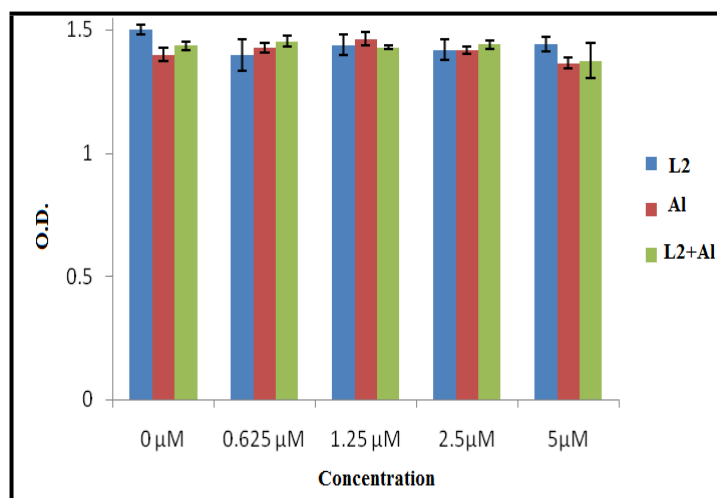


Figure S32. MTT assay to determine the cytotoxic effect of L2 and [Al L2] complex on Vero cell .

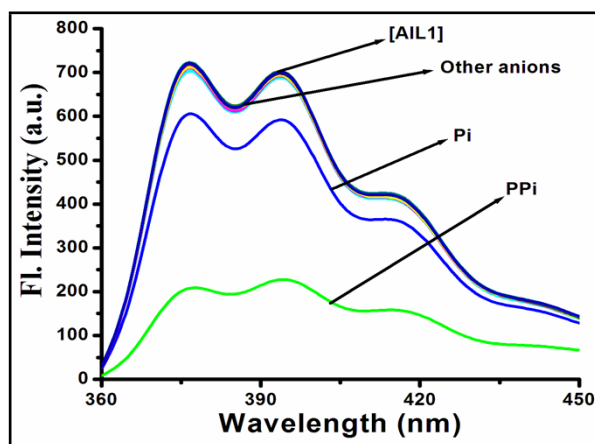


Figure S33. Competitive fluorescence spectra of [AIL1] with different anions(in DMSO-H₂O; 2:1(v/v), HEPES buffer of pH 7.4).

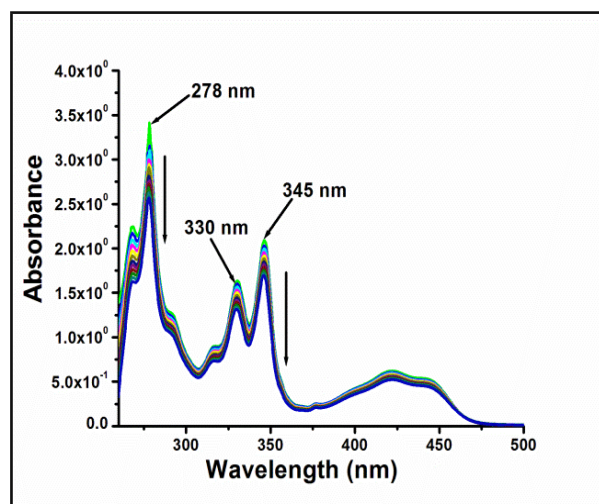


Figure S34. . UV-vis spectral changes of L3 (2.0×10^{-5} M) in DMSO-H₂O (2:1, v/v; pH 7.4) upon addition of Al³⁺ (4.0×10^{-4} M).

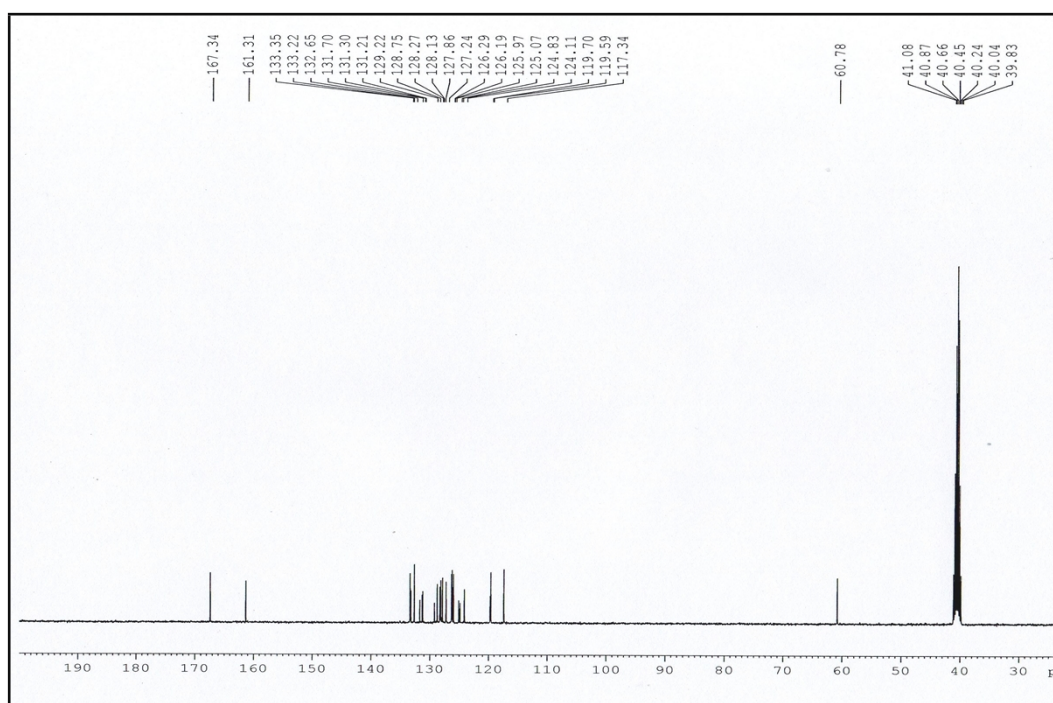


Figure S35. ¹³C NMR spectra of L1.

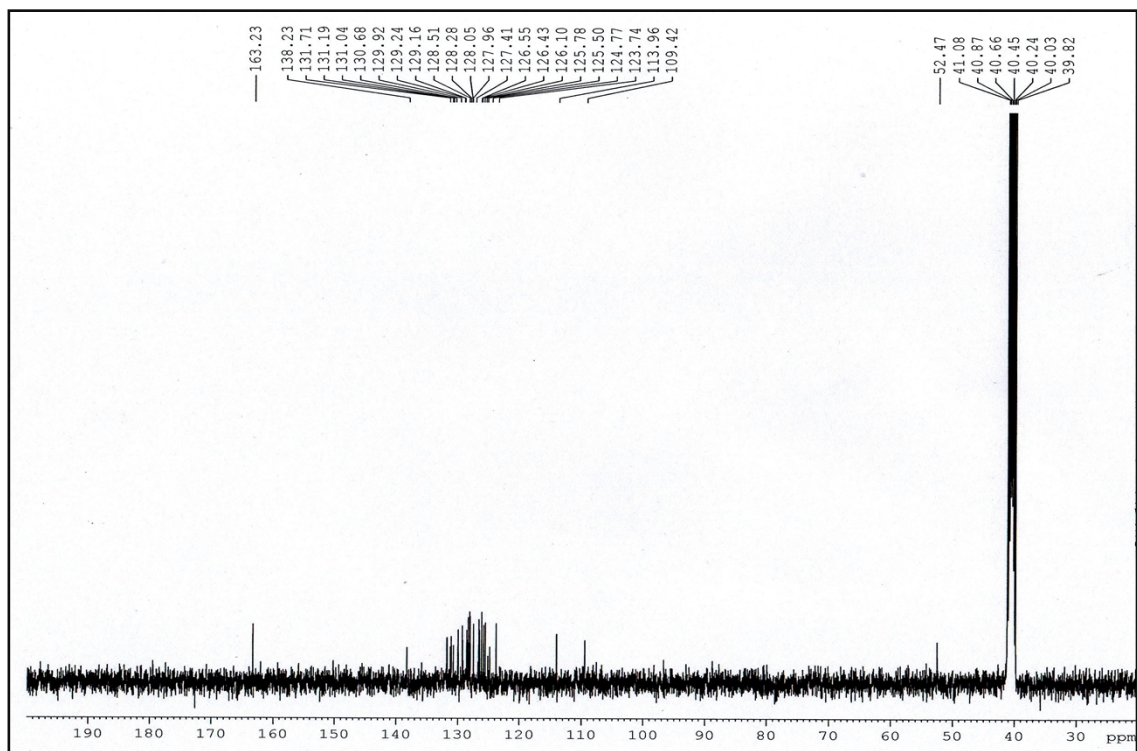


Figure S36. ^{13}C NMR spectra of L3.